JACS
JOURNAL OF THE AMERICAN CHEMICAL SOCIETY
Article
Cite This: J. Am. Chem. Soc. 2019, 141, 363−369
pubs.acs.org/JACS

Transition of Metastable Cross-α Crystals into Cross-β Fibrils by β-Turn Flipping

Sudipta Mondal,[†] Guy Jacoby,[‡] Michael R. Sawaya,[§] Zohar A. Arnon,[†] Lihi Adler-Abramovich,[∥] Pavel Rehak,[⊥] Lela Vuković,[#] Linda J. W. Shimon,[¶] Petr Král,[⊥,□] Roy Beck,[‡] and Ehud Gazit*[,†,△]

[†]Department of Molecular Microbiology and Biotechnology, George S. Wise Faculty of Life Sciences, Tel Aviv University, Tel Aviv 69978, Israel

[‡]The Raymond and Beverly Sackler School of Physics and Astronomy, Tel Aviv University, Tel Aviv 69978, Israel

[§]Howard Hughes Medical Institute, UCLA-DOE Institute, Departments of Biological Chemistry and Chemistry and Biochemistry, Box 951570, UCLA, Los Angeles, California 90095-1570, United States

[∥]Department of Oral Biology, The Goldschleger School of Dental Medicine, Tel Aviv University, Tel Aviv 69978, Israel

[⊥]Department of Chemistry, University of Illinois at Chicago, Chicago, Illinois 60607, United States

[#]Department of Chemistry, University of Texas at El Paso, El Paso, Texas 79968, United States

[¶]Department of Chemical Research Support, Weizmann Institute of Science, Rehovot 76100, Israel

[□]Department of Biopharmaceutical Sciences, University of Illinois at Chicago, Chicago, Illinois 60607, United States

[△]Department of Materials Science and Engineering, Iby and Aladar Fleischman Faculty of Engineering, Tel Aviv University, Tel Aviv 69978, Israel

Supporting Information

ABSTRACT: The ensemble of native, folded state was once considered to represent the global energy minimum of a given protein sequence. More recently, the discovery of the cross-β amyloid state revealed that deeper energy minima exist, often associated with pathogenic, fibrillar deposits, when the concentration of proteins reaches a critical value. Fortunately, a sizable energy barrier impedes the conversion from native to pathogenic states. However, little is known about the structure of the related transition state. In addition, there are indications of polymorphism in the amyloidogenic process. Here, we report the first evidence of the conversion of metastable cross-α-helical crystals to thermodynamically stable cross-β-sheet-like fibrils by a *de novo* designed heptapeptide. Furthermore, for the first time, we demonstrate at atomic resolution that the flip of a peptide plane from a type I to a type II′ turn facilitates transformation to cross-β structure and assembly of a dry steric zipper. This study establishes the potential of a peptide turn, a common protein secondary structure, to serve as a principal gatekeeper between a native metastable folded state and the amyloid state.

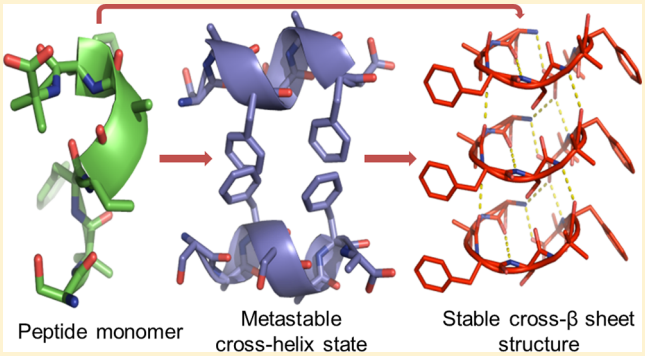

INTRODUCTION

The aggregation of many intrinsically disordered as well as globular proteins into insoluble fibrillar deposits with cross-β architecture is the hallmark of various debilitating pathologies, including Alzheimer's, Parkinson's, and Huntington's diseases.[1−4] Critical evidence suggests that several of the natively unfolded sequences, en route to aggregation, populate an intermediate oligomeric state rich in helix−helix associations, whereas the intermediate state of globular proteins proceeds via assembly of partially unfolded native-like structures and many of them have helical conformation.[5−8] In a pioneering work, Dobson and co-workers demonstrated that myoglobin, a predominantly α-helical globular protein, not related to any known disease conditions, converts to amyloid-like fibrillar aggregates with cross-β structure at high pH and elevated temperature.[9] Subsequently, it has been indicated that above a critical concentration the natively folded soluble proteins may be metastable in nature and the corresponding Gibbs free energy may represent a local minimum in the energy profile, whereas amyloid fibrils are lower in energy (and thus more favorable) and may actually represent a global minimum.[10,11] A recent report further suggested that the amyloid state can populate different energy levels with novel structural features and revealed the polymorphism within amyloid species.[12] Proteins can also assemble into crystal lattices composed of

Received: September 23, 2018
Published: December 11, 2018

DOI: 10.1021/jacs.8b10289
J. Am. Chem. Soc. 2019, 141, 363−369

native metastable conformations.[13,14] Thus, an *in situ* characterization of the conformational conversion between the native crystalline and cross-β ensembles is expected to provide important atomic-level insights into the structural factors affecting the relative stability of the metastable and amyloid states and the nature of the transition state.[15−17] However, the inability of intrinsically disordered pathologically relevant sequences to form metastable crystalline assemblies has so far hindered such deliberation. Moreover, the different conditions required for *in vitro* fibril formation and crystallization of natively folded proteins,[1,7,9] in contrast to the constant physiological conditions under which amyloidogenesis progresses *in vivo*,[15,18] also comprise a major obstacle.

Significant advancements toward understanding the structural basis for amyloid formation came from the utilization of minimal amyloidogenic fragments.[19−21] Most notably, the first atomic resolution structure of amyloid cross-β spines was deciphered by microcrystal X-ray diffraction of the GNNQQNY heptapeptide, a truncated sequence of the prion-determining domain of the yeast protein Sup35.[22] Recently, Mezzenga and co-workers studied several homologous hexapeptides demonstrating that amyloid crystals, rather than amyloid fibrils, represent the true thermodynamic minima.[23] Yet, a peptide aggregation system delineating the atomic details of both the metastable state and amyloid fibers, formed under physiologically relevant conditions and separated only by the time scale of aggregation, is still unavailable. Here, using a *de novo* designed heptapeptide sequence, we report the first real-time observation and atomic resolution evidence of the conversion of a metastable cross-α-helical crystal into cross-β-like crystalline fibers. Furthermore, these experiments allowed us to examine the role of the peptide turn, a common structural feature in a protein loop, in determining the transition of a native peptide into an amyloid structure.

RESULTS AND DISCUSSION

Recently, we have demonstrated the ability of a short seven-residue sequence, SHR-FF, to self-assemble into crystalline supramolecular fibrillar structures (Figure 1a).[24] To gain further insight into the atomistic features of the SHR-FF fibrillar assembly, we performed X-ray powder diffraction (PXRD) analysis of the lyophilized fiber assemblies (Figure 1b). Furthermore, to eliminate the possibility of structural reorganization during drying, the wide-angle X-ray scattering (WAXS) spectra of the self-assembled nanofibers were also recorded in their original mother liquor without lyophilization. The PXRD and WAXS analyses revealed the same diffraction profiles, both distinctly different from the predicted PXRD pattern of the reported X-ray crystal structure (Figure 1b).[24] The SHR-FF crystal was regrown under conditions native to fibril assemblies as shown in Figure 1c.

Single-crystal X-ray structural analysis revealed that the peptide adopted an amphiphilic helical conformation, with adjacent helical molecules interacting through π-stacking and hydrophobic interactions, as reported earlier.[24] These columnar helical dimeric associations propagated along the *c*-axis and were positioned perpendicular to the length of the crystal (along the *a*-axis), revealing distinct cross-α architecture, as determined by face indexing of the single crystal (Figure 1c and Figure S1). This architecture is similar to a recently reported cross-α structure, though comprised of much shorter peptides.[25,26] The Fourier-transform infrared spectroscopy (FTIR) signal of the dried crystals at 1658 cm^{-1} also

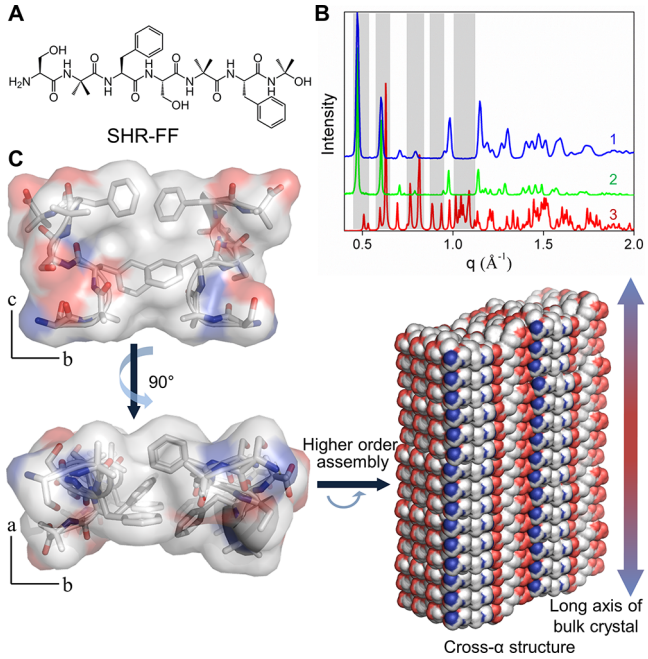

Figure 1. Supramolecular helical organization of SHR-FF. (a) Chemical structure of the SHR-FF heptapeptide. (b) Experimental WAXS (1) and PXRD (2) profiles of SHR-FF and a predicted PXRD pattern (3) generated from the crystal structure shown in (c). Major differences in peaks are highlighted with shaded bars. (c) Single-crystal X-ray analysis of cross-α architecture of SHR-FF viewed parallel (top) and perpendicular (bottom, represented as solvent-accessible surface) to the length of the crystal. Blue and red denote positively and negatively charged surfaces, respectively, and gray denotes a hydrophobic surface.

supported the helical conformation (Figure S1). Since a cross-α structure cannot account for the observed X-ray scattering profile, it was concluded that SHR-FF could adopt two distinct higher order self-assembled states. Additional WAXS analysis established that the formation of a noncross-α fibrillar state does not depend on the cosolvent or buffer compositions (Figure S2).

To distinguish the boundaries between the two phases of SHR-FF and ascertain their morphological differences, freshly prepared SHR-FF solutions (5 mg mL^{-1}) were assembled at different temperatures. Consistent with our diffraction studies, two distinct types of self-assembled structures were evident by optical and transmission electron microscopy (Figures 2a,b and S3). At a low temperature (4 °C), SHR-FF assembly was dominated by elongated flat tape-like microstructures, whereas at a relatively elevated temperature (30 °C), it formed nanofibers. We used microcrystal diffraction techniques to determine the atomic structure of the fibrillar assembly (Figure 2c). Unlike the cross-α structure, the dihedral angles of the peptide backbones, except for the α-aminoisobutyric acid residues, reside in the allowed β-sheet region (Table S1). SHR-FF adopted a looplike conformation highly resembling the loop region of the atomic model of amyloid-β (1−42) fibrils derived from NMR[27] as well as cryo-electron microscopy studies[28] (Figures 2c and S4). In contrast to cross-α assembly, the SHR-FF strand formed a single intramolecular amide hydrogen bond between serine and phenylalanine located near the N-terminus, thus constituting a type II′ β-turn. The adjacent SHR-FF strands were parallel and exactly in register, as seen in the Aβ fibrils[28] and in the atomic structure of the

DOI: 10.1021/jacs.8b10289
J. Am. Chem. Soc. 2019, 141, 363−369

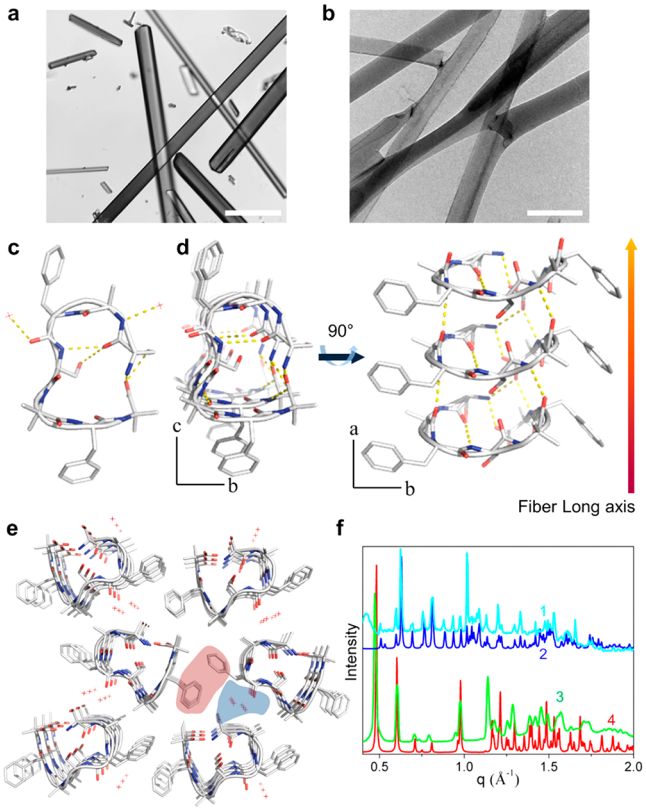

Figure 2. Separation and characterization of different crystalline phases. SHR-FF self-assembled structures at (a) 4 °C (scale bar, 50 μm) and (b) 30 °C (scale bar, 200 nm). (c) Asymmetric unit observed in the single-crystal X-ray analysis of the stable phase of SHR-FF. The H-bondings are shown as yellow dotted lines. (d) View of the packing of SHR-FF at a parallel (left) and perpendicular (right) orientation relative to the long axis of the fibril. (e) The crystal lattice exhibits distinct dry (red area) and wet interfaces (blue area). Water molecules are marked as red plus signs. (f) Comparison of the WAXS profiles of the cross-α (1, experimental; 2, predicted) and cross-β (3, experimental; 4, predicted) structures with the predicted PXRD data obtained from the corresponding single-crystal X-ray analysis, respectively.

amyloid cross-β spine[22] (Figure 2d). The β-sheet-like layered structure is stabilized by intermolecular amide H-bonding and parallel-displaced stacking interactions involving phenylalanine side chains, which play an important role in Aβ aggregation.[29] The individual sheet organized parallel to the fibril axis, thus revealing a cross-β-like architecture (Figures 2d and S1). The crystal lattice also exhibited distinct dry and wet interfaces as observed in the crystals of amyloid-derived protein segments (Figure 2e, red and blue areas, respectively).[22] The dry interfaces were stabilized by phenylalanine zipper and hydrophobic interactions (Figure S5). Such a complementary dry steric zipper is considered to be a fundamental structural unit that provides exceptional stability to amyloid fibrils.[19] The WAXS profiles of flat tape structures and the nanofiber morphology showed an excellent correlation with the predicted PXRD pattern of cross-α and cross-β crystals, respectively, confirming the existence of two different SHR-FF ensembles corresponding to the two basic secondary structure modules (Figure 2f). The atomic level structural similarity of cross-β-like SHR-FF fibers to amyloid aggregates prompted us to study the functional attributes of SHR-FF fibrillar aggregates. As expected, these fibrils were highly stable, bound to the amyloid specific dye thioflavin T, and displayed nucleated polymerization-like growth kinetics, a hallmark of amyloid fibrils (Figure S6).

The finding that SHR-FF can alternatively exist as cross-α or cross-β-like ensembles separated only by a thermal energy barrier could serve as a paradigm for delineation of assembly kinetics of two basic secondary structure modules. To understand the relationship between the two ensembles states, we prepared cross-α crystals at 4 °C and measured their WAXS spectra at different temperatures over time. As shown in Figure 3a, the cross-α phases showed substantial stability at 37 °C, but rapidly converted to cross-β-like structures and remained stable when heated to 50 °C. The complete conversion of cross-α crystal to cross-β fibrils confirmed that the former represents a metastable state, a generic feature of native polypeptide and protein assemblies. Further evidence for the metastable nature of a cross-α phase was obtained by measuring the equilibrium concentration of peptide monomers in solution, showing the cross-β-fibrils to be more stable than the native cross-α structures by 3.3 kJ mol^{-1}, as illustrated in the energy profile diagram (Figures 3b and S7).

In order to gain more insight into the relative stabilities of alpha helical and non-alpha helical peptide structures in free and crystalline forms, we modeled these systems by atomistic molecular dynamics (MD) simulations. First, we simulated 10 separated peptides solvated in a physiological solution at temperatures of 37, 50, and 70 °C. Every 10 ps, we calculated RMSDs of all peptides best aligned with respect to the alpha helical and non-alpha helical forms, taken from their crystalline structures, and obtained a 2D histogram of their relative populations. Figure 3c shows the distribution of RMSDs for freely solvated peptides at 37 °C; distributions for higher temperatures are shown in Figure S8. Each distribution has two main populations of peptide conformations for the helical (major) and non-helical (minor) conformations. As seen in Table S2 and Figures 3c and S8, as temperature increases, the population of helical conformation decreases and the non-helical increases. There is a dramatic change of 10% from 37 to 50 °C, but only a slight change of 1% from 50 to 70 °C; 90–95% of all peptides are always within these two regions. The obtained results reveal that freely solvated peptides are significantly more likely to assume conformations resembling the helical (crystal) form than the non-helical form. At higher temperatures there is a stronger presence of peptides in non-alpha helical form because it is entropically favored.

Finally, we simulated Cross-α and Cross-β crystallites with 12 × 12 × 12 peptides (Note S1). On each facet, we allowed the central 10 × 10 peptides to freely diffuse, while the remaining peptides in the crystal were frozen. We calculated RMSDs of each free peptide (best match) with respect to its initial conformation. Figure 3d shows the evolution of RMSDs averaged over the 100 respective peptides. Among the six observed RMSD dependencies, peptides on two non-helical and (partly) one helical facets largely preserve their initial conformations, revealing that in the crystalline form the Cross-β structure might be more stable than the Cross-α structure.

Next, we analyzed the structural reorganization in real time by heating the SHR-FF helical ensembles, replicating the WAXS kinetic experimental conditions. At 37 °C, all the crystals grew in size via addition of monomers to the crystal surfaces and maintained stability more than 12 h (Figure 3e and Video S1). Upon increasing the temperature to 50 °C, the crystals underwent dissolution by dissipating the monomers

DOI: 10.1021/jacs.8b10289
J. Am. Chem. Soc. 2019, 141, 363−369

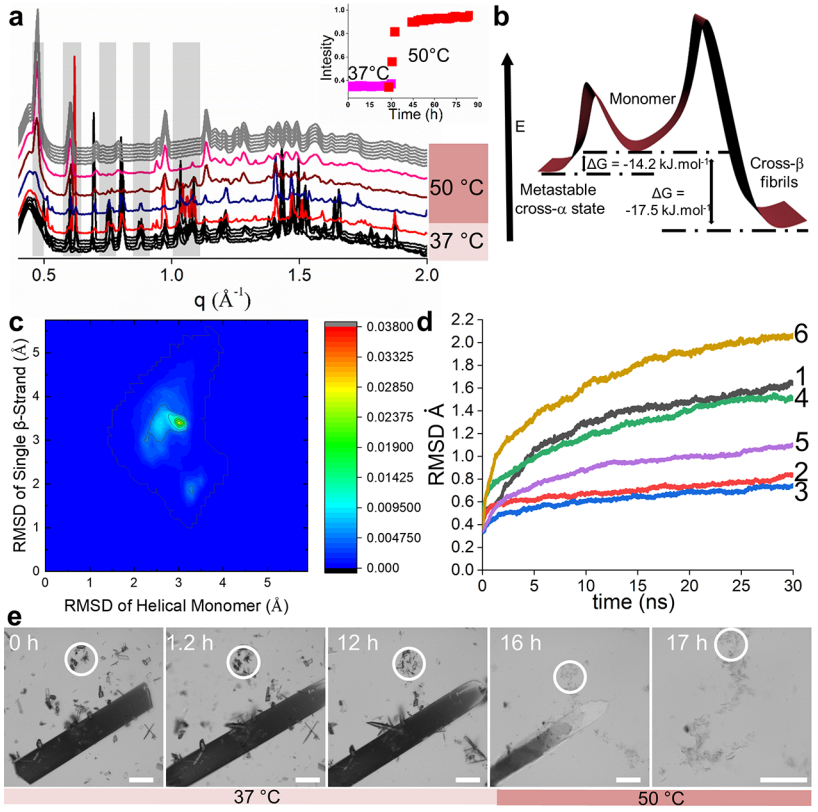

Figure 3. Kinetic studies of cross-α to cross-β-like structural conversion. (a) Real-time WAXS analysis of the conversion from the cross-α to cross-β fibrillar state. The cross-α crystals persisted at 37 °C (black curves) and showed a sharp transition (colored curves) into the stable cross-β structure (gray curves) upon increasing the temperature to 50 °C. Major differences in peaks are highlighted with a shaded bar. The data sets are vertically offset. Inset: Kinetic profile of fibrils assembly generated by plotting the peak intensity at 0.475 Å^{-1} versus time. The temperatures corresponding to different measurements are shaded with two different colors. (b) Schematic representation of the free energy profile of the metastable cross-α crystals and thermodynamically stable cross-β like fibrils. (c) A 2-D histogram of RMSDs for 10 solvated peptides (90 ns) evaluated with respect to their helical and β-strand-like conformations. The analysis was performed for 90 000 snapshots of individual peptides. Density = (counts/90 000). (d) RMSDs of 100 peptides averaged for each crystal facet of two crystalline structures (1−3 represent cross-β facets and 4−6 represent cross-helix facets, respectively). (e) Progressive images of the fibril formation (white circle) from the dissolution of metastable cross-α crystals on increasing the temperature from 37 to 50 °C (scale bar, 100 μm).

into the solution, whereas a subsection of the metastable structures transitioned into fibers in a spatially correlated region, as marked by a white circle in Figure 3e (Video S2). This observation indicated that the nucleation of the cross-β oligomers occurred in the region with the highest peptide concentration and subsequently elongated, in accordance with a nucleated polymerization-like model. The kinetic profile delineated by real-time optical microscopy analysis correlated precisely with the WAXS kinetics (Figure 3a). The sharp transition in WAXS spectra during the heating process also supported the nucleated polymerization-like growth (inset, Figure 3a). In addition, we studied the kinetics of fibril formation starting from metastable cross-α crystals, and it afforded almost the same kinetic profile as if the aggregation was initiated from peptide monomers (Figure S6). Most importantly, the cross-α to cross-β transition did not require an increased temperature, but could proceed at constant conditions in a time-dependent manner, thus resembling the pathological amyloid aggregation. At a constant 30 °C temperature, the conversion required 7−8 days, as compared to several at 50 °C. At 4 °C, the time scale was further prolonged to 10−12 months (Figure S9).

Most peptides and proteins can be coaxed under certain conditions to assemble into amyloid fibrils; however a particular structural rearrangement that accompanies this transformation has not been identified. High-resolution X-ray crystal structures of both the metastable helical assembly and thermodynamically stable cross-β fibrils allowed us to decipher the structural features involved in amyloid aggregation in atomic detail. Analysis of the structures revealed that the N-terminal regions of both helical and cross-β assemblies have similar backbone and side chain conformations, stabilized by a conserved i to i + 3 H-bond (Figure 4a). The conformation is classified as a type I turn in the helical assembly and a type II′ turn in the cross-β assembly, as specified by their respective dihedral angles (Figure 4b). Such a peptide−plane-flip, in which the conformation of a central peptide module changes from one allowed structural region to a different one without breaking intramolecular i to i + 3 H-bonding has been identified in many homologous protein crystal structures.[30] However, peptide flip, as described here for SHR-FF, can transform a native backbone conformation into an amyloidogenic one. The important role of plane-flip in natural amyloidosis is also evident by the fact that the amino acid residues most prone to turn-flip,[15] namely, proline, lysine, glycine, serine, and asparagine, were primarily found in the loop region of the atomic resolution structures of amyloid-β and Tau fibrils associated with Alzheimer's disease.[28,31] In

DOI: 10.1021/jacs.8b10289
J. Am. Chem. Soc. 2019, 141, 363−369

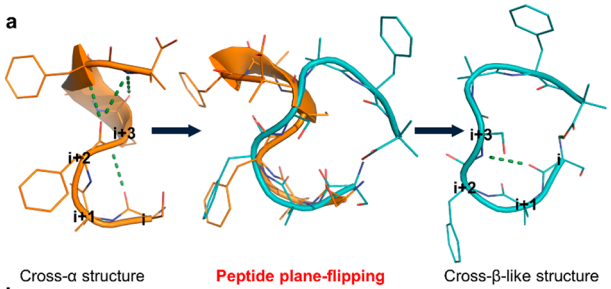

b

Residues	Cross-α crystals Type I turn		Cross-β-like fibrils Type II′ turn	
	φ	ψ	φ	ψ
i	-	-	-	-
i+1	-51.3	-37.6	46.7	-130.7
i+2	-98.9	22.9	-96.1	5.2
i+3	-	-	-	-

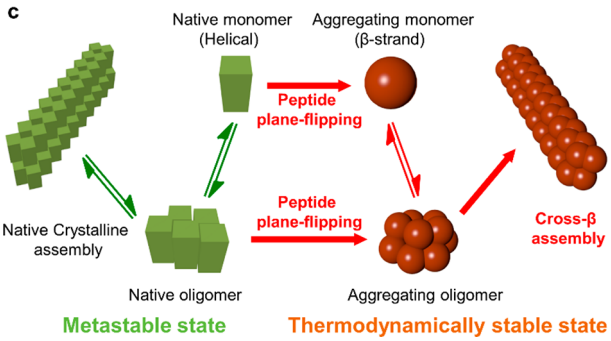

Figure 4. Atomistic details of cross-α to cross-β structural transition. (a) Active flipping of peptide planes from type I to type II′ β-turn. Residues associated with plane flip are labeled as i to i + 3. (b) Changes in the dihedral angles of the key i + 1 and i + 2 residues during the transition from helical to β-sheet structure. (c) Schematic illustration of the possible transformation mechanism of native helical peptide conformation into cross-β fibrils by β-turn peptide plane-flipping.

addition, this observation also suggests a solution to the conundrum associated with the binding of oligomer specific antibody to all types of soluble oligomers prepared from amyloid related proteins or peptides irrespective of the sequences.[19] Consistently, the turn represents a very common secondary structure, and the turn-forming sequence having the potential to flip is composed of a limited number of amino acids common to many amyloidogenic peptides as discussed above.

The transformation of native helical peptide structures to their cross-β assembly can be summarized as depicted in Figure 4c. In a solution, SHR-FF exists mainly in a helical conformation, as reported before[24] and validated by MD simulations. The facile conversion from a metastable crystalline to fibrils state was observed in the temperature ranges from 4 to 30 °C and 50 °C, reached with a decreasing time duration (Figure S9). The results indicate the formation of a metastable helical oligomer in the early stages of nucleation, which subsequently converts to the aggregation-prone oligomer by a peptide plane-flipping. In addition, the concentration-dependent kinetic assay provided further evidence for this process. As shown in Figure S10, at a concentration of 5 mg mL^{-1}, the kinetics of cross-β fibril formation starting from either a monomer or a cross-α crystalline structure comprised a comparable $t_{1/2}$. However, at a lower concentration (3 mg mL^{-1}), the kinetics of cross-β fibril formation starting from a cross-α crystalline structure was notably faster than the same process starting from the monomer. Thus, the presence of preformed cross-helical nuclei reduced the overall $t_{1/2}$ of SHR-FF assembly into cross-β fibrils, consistent with the fact that the nucleation event is a rate-limiting process. Alternatively, the conversion of type I to type II′ turn may proceed in the monomeric state at higher temperatures (50 °C), where the nonhelical peptide monomers may be more stable due to entropic reasons (more open structure). It is important to mention that the complete conversion of the metastable helical conformation into cross-β fibrils may involve multiple energy barriers, which are common in protein folding and amyloid aggregation.[12] These cross-β oligomers underwent further elongation, with the conformational conversion possibly catalyzed by cross-β oligomers or fibrils, in which metastable helical assemblies serve as a monomer reservoir, as evident in Figure 3e, a common characteristic of amyloid aggregation.

CONCLUSION

In summary, we have identified a minimal peptide module that, similar to many natural protein or peptide sequences, demonstrates dynamic transformation between native crystalline state and cross-β amyloidal state. This simple system recapitulated the complex amyloid aggregation pattern recognized in Alzheimer's, Parkinson's, and prion diseases. Furthermore, it allowed us to decipher, for the first time, the crucial role of the β-turn, the minimal regular secondary structural motif abundant in both native proteins and amyloid fibrils, as a transient intermediate in peptide aggregation. The energetically favorable transformation between β-turn conformations, permissible in the Ramachandran plot, can convert a native peptide backbone into an amyloidogenic sequence.

The X-ray crystallographic coordinates for structures reported in this study have been deposited in the Cambridge Crystallographic Data Centre (CCDC), under deposition number CCDC 1569244, and in the Protein Data Bank with PDB code 5VSG.

ASSOCIATED CONTENT

Supporting Information

The Supporting Information is available free of charge on the ACS Publications website at DOI: 10.1021/jacs.8b10289.

Crystallographic coordinates of cross-α structure (Data S1) (CIF)

Crystallographic coordinates of cross-β fibrils (Data S2) (CIF)

Structure of cross-β fibrils (Data S2) (PDB)

General sample preparation; crystallization and structure determination; procedures for wide-angle X-ray scattering, transmission electron microscopy, powder X-ray diffraction, optical microscopy studies, kinetic assays, ultraviolet−visible spectroscopy, FTIR spectroscopy, details of MD simulation, and additional discussion (PDF)

Growth of cross-α crystals (video S1) (AVI)

Transition of cross-α crystals to cross-β fibrils (video S2) (AVI)

AUTHOR INFORMATION

Corresponding Author

*ehudg@post.tau.ac.il

ORCID

Sudipta Mondal: 0000-0002-1146-8659

DOI: 10.1021/jacs.8b10289
J. Am. Chem. Soc. 2019, 141, 363−369

Zohar A. Arnon: 0000-0003-2915-5930
Lihi Adler-Abramovich: 0000-0003-3433-0625
Linda J. W. Shimon: 0000-0002-7861-9247
Petr Král: 0000-0003-2992-9027
Roy Beck: 0000-0003-3121-4530
Ehud Gazit: 0000-0001-5764-1720

Notes

The authors declare no competing financial interest.

■ ACKNOWLEDGMENTS

We thank Dr. Vered Holdengreber and Dr. Lubov Burlaka for help with TEM analysis and members of the Gazit laboratory for helpful discussions. This work is based upon research conducted at the Northeastern Collaborative Access Team beamline 24-ID-E, which is funded by the National Institute of General Medical Sciences from the National Institutes of Health (P41 GM103403). The Eiger 16M detector on the 24-ID-E beamline is funded by an NIH-ORIP HEI grant (S10OD021527). This research used resources of the Advanced Photon Source, a U.S. Department of Energy (DOE) Office of Science User Facility operated for the DOE Office of Science by Argonne National Laboratory under Contract No. DE-AC02-06CH11357. S.M. thanks the PBC Program for outstanding Postdoctoral Researchers from China and India and Tel Aviv University for scholarships. P.K. was supported by the NSF DMR-1506886. L.V. was supported by the startup funding from the University of Texas at El Paso. R.B. acknowledges the support from the Israeli Science Foundation (550/15). This project has received funding from the European Research Council (ERC) under the European Union's Horizon 2020 research and innovation program (grant agreement no. BISON-694426 to E.G.). We thank Dr. Sigal Rencus-Lazar for her valuable comments and suggestions. We also thank Prof. David Eisenberg for his critical evaluation of the manuscript.

■ REFERENCES

(1) Chiti, F.; Dobson, C. M. Protein Misfolding, Amyloid Formation, and Human Disease: A Summary of Progress over the Last Decade. *Annu. Rev. Biochem.* **2017**, *86*, 27−68.
(2) Eisele, Y. S.; Monteiro, C.; Fearns, C.; Encalada, S. E.; Wiseman, R. L.; Powers, E. T.; Kelly, J. W. Targeting Protein Aggregation for the Treatment of Degenerative Diseases. *Nat. Rev. Drug Discovery* **2015**, *14* (11), 759−780.
(3) Wong, Y. C.; Krainc, D. α-Synuclein Toxicity in Neurodegeneration: Mechanism and Therapeutic Strategies. *Nat. Med.* **2017**, *23*, 1−13.
(4) Perutz, M. F.; Pope, B. J.; Owen, D.; Wanker, E. E.; Scherzinger, E. Aggregation of Proteins with Expanded Glutamine and Alanine Repeats of the Glutamine-Rich and Asparagine-Rich Domains of Sup35 and of the Amyloid β-Peptide of Amyloid Plaques. *Proc. Natl. Acad. Sci. U. S. A.* **2002**, *99* (8), 5596−5600.
(5) Fiumara, F.; Fioriti, L.; Kandel, E. R.; Hendrickson, W. A. Essential Role of Coiled-Coils for Aggregation and Activity of Q/N-Rich Prions and PolyQ Proteins. *Cell* **2010**, *143* (7), 1121−1135.
(6) Abedini, A.; Raleigh, D. P. A Critical Assessment of the Role of Helical Intermediates in Amyloid Formation by Natively Unfolded Proteins and Polypeptides. *Protein Eng., Des. Sel.* **2009**, *22* (8), 453−459.
(7) Jahn, T. R.; Parker, M. J.; Homans, S. W.; Radford, S. E. Amyloid Formation under Physiological Conditions Proceeds via a Native-like Folding Intermediate. *Nat. Struct. Mol. Biol.* **2006**, *13* (3), 195−201.
(8) Chiti, F.; Dobson, C. M. Amyloid Formation by Globular Proteins under Native Conditions. *Nat. Chem. Biol.* **2009**, *5* (1), 15−22.
(9) Fandrich, M.; Fletcher, M. A.; Dobson, C. M. Amyloid Fibrils from Muscle Myoglobin. *Nature* **2001**, *410* (6825), 165−166.
(10) Gazit, E. The "Correctly Folded" State of Proteins: Is It a Metastable State? *Angew. Chem., Int. Ed.* **2002**, *41* (2), 257−259.
(11) Baldwin, A. J.; Knowles, T. P. J.; Tartaglia, G. G.; Fitzpatrick, A. W.; Devlin, G. L.; Shammas, S. L.; Waudby, C. A.; Mossuto, M. F.; Meehan, S.; Gras, S. L.; Christodoulou, J.; Anthony-Cahill, S. J.; Barker, P. D.; Vendruscolo, M.; Dobson, C. M. Metastability of Native Proteins and the Phenomenon of Amyloid Formation. *J. Am. Chem. Soc.* **2011**, *133* (36), 14160−14163.
(12) Adamcik, J.; Mezzenga, R. Amyloid Polymorphism in the Protein Folding and Aggregation Energy Landscape. *Angew. Chem., Int. Ed.* **2018**, *57* (28), 8370−8382.
(13) Schlichting, I.; Berendzen, J.; Phillips, G. N.; Sweet, R. M. Crystal Structure of Photolysed Carbonmonoxy-Myoglobin. *Nature* **1994**, *371* (6500), 808−812.
(14) Trinh, C. H.; Smith, D. P.; Kalverda, A. P.; Phillips, S. E. V.; Radford, S. E. Crystal Structure of Monomeric Human Beta-2-Microglobulin Reveals Clues to Its Amyloidogenic Properties. *Proc. Natl. Acad. Sci. U. S. A.* **2002**, *99* (15), 9771−9776.
(15) Fusco, G.; Chen, S. W.; Williamson, P. T. F.; Cascella, R.; Perni, M.; Jarvis, J. A.; Cecchi, C.; Vendruscolo, M.; Chiti, F.; Cremades, N.; Ying, L.; Dobson, C. M.; De Simone, A. Structural Basis of Membrane Disruption and Cellular Toxicity by α-Synuclein Oligomers. *Science* **2017**, *358* (6369), 1440−1443.
(16) Neudecker, P.; Robustelli, P.; Cavalli, A.; Walsh, P.; Lundström, P.; Zarrine-Afsar, A.; Sharpe, S.; Vendruscolo, M.; Kay, L. E. Structure of an Intermediate State in Protein Folding and Aggregation. *Science* **2012**, *336* (6079), 362−366.
(17) Karamanos, T. K.; Kalverda, A. P.; Thompson, G. S.; Radford, S. E. Visualization of Transient Protein-Protein Interactions That Promote or Inhibit Amyloid Assembly. *Mol. Cell* **2014**, *55* (2), 214−226.
(18) Krishnan, R.; Goodman, J. L.; Mukhopadhyay, S.; Pacheco, C. D.; Lemke, E. A.; Deniz, A. A.; Lindquist, S. Conserved Features of Intermediates in Amyloid Assembly Determine Their Benign or Toxic States. *Proc. Natl. Acad. Sci. U. S. A.* **2012**, *109* (28), 11172−11177.
(19) Sawaya, M. R.; Sambashivan, S.; Nelson, R.; Ivanova, M. I.; Sievers, S. A.; Apostol, M. I.; Thompson, M. J.; Balbirnie, M.; Wiltzius, J. J. W.; McFarlane, H. T.; Madsen, A. Ø.; Riekel, C.; Eisenberg, D. Atomic Structures of Amyloid Cross-Beta Spines Reveal Varied Steric Zippers. *Nature* **2007**, *447* (7143), 453−457.
(20) Rodriguez, J. A.; Ivanova, M. I.; Sawaya, M. R.; Cascio, D.; Reyes, F. E.; Shi, D.; Sangwan, S.; Guenther, E. L.; Johnson, L. M.; Zhang, M.; Jiang, L.; Arbing, M. A.; Nannenga, B. L.; Hattne, J.; Whitelegge, J.; Brewster, A. S.; Messerschmidt, M.; Boutet, S.; Sauter, N. K.; Gonen, T.; Eisenberg, D. S. Structure of the Toxic Core of α-Synuclein from Invisible Crystals. *Nature* **2015**, *525* (7570), 486−490.
(21) Stöhr, J.; Wu, H.; Nick, M.; Wu, Y.; Bhate, M.; Condello, C.; Johnson, N.; Rodgers, J.; Lemmin, T.; Acharya, S.; Becker, J.; Robinson, K.; Kelly, M. J. S.; Gai, F.; Stubbs, G.; Prusiner, S. B.; DeGrado, W. F. A 31-Residue Peptide Induces Aggregation of Tau's Microtubule-Binding Region in Cells. *Nat. Chem.* **2017**, *9*, 874−881.
(22) Nelson, R.; Sawaya, M. R.; Balbirnie, M.; Madsen, A. Ø.; Riekel, C.; Grothe, R.; Eisenberg, D. Structure of the Cross-Beta Spine of Amyloid-like Fibrils. *Nature* **2005**, *435* (7043), 773−778.
(23) Reynolds, N. P.; Adamcik, J.; Berryman, J. T.; Handschin, S.; Zanjani, A. A. H.; Li, W.; Liu, K.; Zhang, A.; Mezzenga, R. Competition between Crystal and Fibril Formation in Molecular Mutations of Amyloidogenic Peptides. *Nat. Commun.* **2017**, *8* (1), 1338.
(24) Mondal, S.; Adler-Abramovich, L.; Lampel, A.; Bram, Y.; Lipstman, S.; Gazit, E. Formation of Functional Super-Helical Assemblies by Constrained Single Heptad Repeat. *Nat. Commun.* **2015**, *6*, 8615.

DOI: 10.1021/jacs.8b10289
J. Am. Chem. Soc. 2019, 141, 363−369

(25) Tayeb-Fligelman, E.; Tabachnikov, O.; Moshe, A.; Goldshmidt-Tran, O.; Sawaya, M. R.; Coquelle, N.; Colletier, J.-P.; Landau, M. The Cytotoxic Staphylococcus Aureus PSMα3 Reveals a Cross-α Amyloid-like Fibril. *Science* **2017**, *355* (6327), 831−833.
(26) Zhang, S.-Q.; Huang, H.; Yang, J.; Kratochvil, H. T.; Lolicato, M.; Liu, Y.; Shu, X.; Liu, L.; DeGrado, W. F. Designed Peptides That Assemble into Cross-α Amyloid-like Structures. *Nat. Chem. Biol.* **2018**, *14* (9), 870−875.
(27) Lührs, T.; Ritter, C.; Adrian, M.; Riek-Loher, D.; Bohrmann, B.; Döbeli, H.; Schubert, D.; Riek, R. 3D Structure of Alzheimer's Amyloid-β(1−42) Fibrils. *Proc. Natl. Acad. Sci. U. S. A.* **2005**, *102* (48), 17342−17347.
(28) Gremer, L.; Schölzel, D.; Schenk, C.; Reinartz, E.; Labahn, J.; Ravelli, R. B. G.; Tusche, M.; Lopez-Iglesias, C.; Hoyer, W.; Heise, H.; Willbold, D.; Schröder, G. F. Fibril Structure of Amyloid-β(1−42) by Cryo−Electron Microscopy. *Science* **2017**, *358* (6359), 116−119.
(29) Reches, M.; Gazit, E. Casting Metal Nanowires within Discrete Self-Assembled Peptide Nanotubes. *Science* **2003**, *300* (5619), 625−627.
(30) Gunasekaran, K.; Gomathi, L.; Ramakrishnan, C.; Chandrasekhar, J.; Balaram, P. Conformational Interconversions in Peptide β-Turns: Analysis of Turns in Proteins and Computational Estimates of Barriers. *J. Mol. Biol.* **1998**, *284* (5), 1505−1516.
(31) Fitzpatrick, A. W. P.; Falcon, B.; He, S.; Murzin, A. G.; Murshudov, G.; Garringer, H. J.; Crowther, R. A.; Ghetti, B.; Goedert, M.; Scheres, S. H. W. Cryo-EM Structures of Tau Filaments from Alzheimer's Disease. *Nature* **2017**, *547*, 185−190.

DOI: 10.1021/jacs.8b10289
J. Am. Chem. Soc. 2019, 141, 363−369